EAS Muon Arrival Time Distributions Measured in the KASCADE Experiment

I.M. Brancus[1*], T. Antoni[2], W.D. Apel[2], A.F. Badea[1], K. Bekk[2], K. Bernlöhr[2], E. Bollmann[2], H. Bozdog[1], A. Chilingarian[3], K. Daumiller[4], P. Doll[2], J. Engler[2], F. Feßler[2], M. Föller[2] H.J. Gils[2], R. Glasstetter[4], R. Haeusler[2 †], W. Hafemann[2], A. Haungs[2], D. Heck[2], T. Holst[2], J.R. Hörandel[2] K.-H. Kampert[2,4], J. Kempa[5], H.O. Klages[2], J. Knapp[4] H.J. Mathes[2], H.J. Mayer[2], J. Milke[2], D. Mühlenberg[2], J. Oehlschläger[2], M. Petcu[1], U. Raidt[2] H. Rebel[2], M. Risse[2], M. Roth[2], G. Schatz[2] F.K. Schmidt[4], T. Thouw[2], H. Ulrich[2], A. Vardanyan[3], B. Vulpescu[1], J. Weber[4], J. Wentz[2], T. Wibig[5], T. Wiegert[2], D. Wochele[2], J. Wochele[2], J. Zabierowski[6], S. Zagromski[2],

[1]*National Institute of Physics and Nuclear Engineering, Bucharest, Romania*

[2]*Forschungszentrum Karlsruhe, Institut für Kernphysik, D-76021 Karlsruhe, Germany*

[3]*Cosmic Ray Division, Yerevan Physics Institute, Yerevan, Armenia*

[4] *Institut für Experimentelle Kernphysik, University of Karlsruhe, Germany*

[5]*University of Lodz, Institute of Physics, Lodz, Poland*

[6] *Soltan Institute for Nuclear Studies, Lodz, Poland*

Abstract

The temporal structure of the EAS muon component, given by median, first and third quartile of the single distributions is studied with the muon detection facilities of the KASCADE central detector. Data have been analysed for EAS core distances up to 130 m and for primary energies of the knee region. The EAS muon time profile and disc thickness have been studied along their dependence on the angle-of-incidence and on the energy indicative muon number N_μ^{tr}, particular attention is paid to which extent EAS muon arrival time distributions at larger radial distances display features indicating a change of the mass composition of primary cosmic rays around the knee. The experimental results are compared with EAS Monte-Carlo (CORSIKA - CRES) simulations including the detector response.

1 Experimental setup and general procedures:

Using the timing and muon detection facilities of the KASCADE central detector (Klages et al., 1997), in particular the trigger layer of 456 scintillation detectors (placed as the third active layer of the hadron calorimeter) and the position sensitive large area multiwire proportional chambers (MWPC) installed below the hadron calorimeter, the muon arrival time distributions ($E_\mu \geq 2$ GeV) have been measured. Their dependence on different shower quantities: the distance from the shower center R_μ, the zenith angle θ of the shower incidence and the muon shower content N_μ^{tr} (representing the muon content with $E_\mu > 250$ MeV, integrated in a limited range of 40 - 200 m from the centre of the lateral muon distribution and considered as an identifier of the primary energy) have been studied (Brancus et al., 1998). The total number of collected events amounts to c. 200 000 with the requirement that at least 3 timing detectors of the timing facility of the central detector must have fired per event. The muon component at energies > 2 GeV is measured as correlated signals of the trigger layer and the MWPC and associated by the general KASCADE trigger to an EAS event.

Measurements of the relative muon arrival time refer to an experimentally defined zero-time, usually the arrival time τ_{cor} of the shower core. These quantities are called *global times* furtheron:

$$\Delta\tau_1^{glob} = \tau_\mu^1 - \tau_{\rm cor}, \tag{1}$$

τ_μ^1 being the arrival time of the foremost muon. The global times are affected by the limited accuracy of the reconstruction procedures of the arrival time of the electromagnetic component, hence we prefer to analyse

*corresponding author; e-mail: iliana@muon2.nipne.ro

†presenting author

local times which refer to the arrival time of the foremost muon, registrated in the timing detector at a particular distance from the center R_μ, defined in a plane perpendicular to the shower axis:

$$\Delta\tau^{loc}(R_\mu) = \tau_\mu(R_\mu) - \tau^1_\mu(R_\mu) \tag{2}$$

We characterize the single local arrival time distributions by different moments T: *the median* ($\Delta\tau_{0.50}$), *the first* and *the third quartile* ($\Delta\tau_{0.25}$ and $\Delta\tau_{0.75}$). In order to supress faked muons from hadron events (noticeable at $R_\mu \leq 30$ m), a condition for the energy deposit in the scintillator detectors has been applied.

2 The EAS muon shower profile and disc thickness:

We consider the muon arrival time distributions in different intervals of the core distance $R_\mu = 20 - 30$ m, ... up to 130 m for different ranges of zenith angles and for 5 ranges of the $\log_{10} N^{tr}_\mu$. From the local arrival time distributions determining the mean values and the standard deviations one obtaines the muon shower profile and the disc thickness.

Fig. 1 presents the variation of the median muon arrival time distributions with the distance from the shower core, compared with a description by a Γ-probability distribution function (Woidneck et al., 1975):

$$\Gamma(T) = aT^b exp(-cT) \tag{3}$$

with a mean value $T(R_\mu) = (1+b)/c$ and the standard deviation $\sigma^\Gamma = (1+b)^{1/2}/c$.

It is obvious that the muon arrival time distributions become broader with increasing radial distances and narrower with increasing $\log_{10} N^{tr}_\mu$ size.

Fig. 2 shows the muon shower profile and the disc thickness comparing the mean values and the standard deviations extracted directly from the experimental (histograms) distributions for different $\log_{10} N^{tr}_\mu$ to those fitted by a Γ-Form. The shape of the EAS profile has been approximated by a parabolic form (Ambrosio et al., 1997):

$$T(R_\mu) = t_1 + t_2(R_\mu/R_m)^\beta \tag{4}$$

with $R_m = 100$ m, the scaling radius for muon lateral distribution. Some limitations of the used parametrization are observed, in particular for the variances of the slower

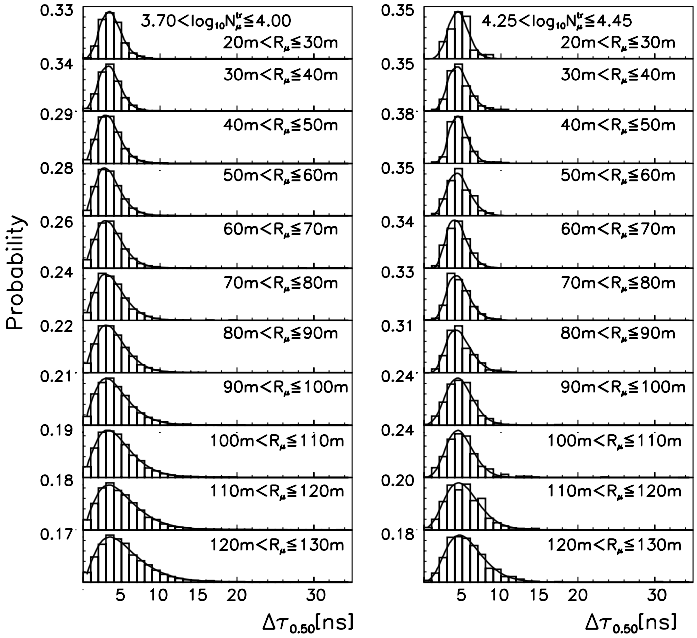

Figure 1: The variation of the shape of the median distribution with the core distance R_μ for two $\log_{10} N^{tr}_\mu$ ranges and for $5^o < \theta \leq 30^o$. The distributions are normalised to the maximum number of particle per time-bin. The lines give the fits by the Γ-form.

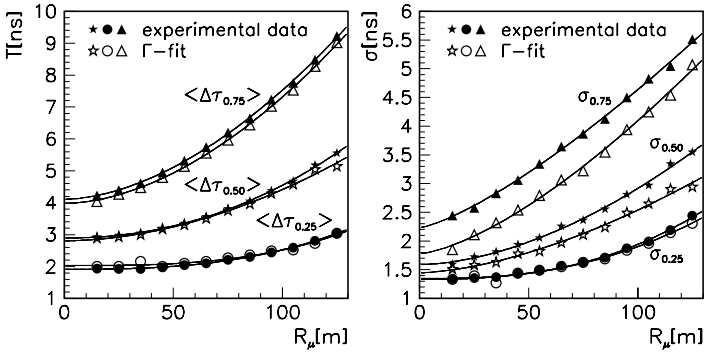

Figure 2: The mean values and standard deviations of the median, first and third quartiles distributions extracted from the distributions (Fig. 1) and compared with those from fitting the distributions with a Γ- form

muon component, but the deviations are much smaller than that observed for the charged particle component (Agnetta et al., 1997).

3 The variation of the muon shower profile with N_μ^{tr}:

As Monte-Carlo simulations show, for the KASCADE experiment the quantity $\log_{10} N_\mu^{tr}$ is approximately proportional $\log_{10} E_0$ and independent from the primary mass. Thus the use of EAS classification along $\log_{10} N_\mu^{tr}$ instead of $\log_{10} N_e$ avoids preparing samples mixing different energy ranges of different primary masses (Haungs et al., 1998).

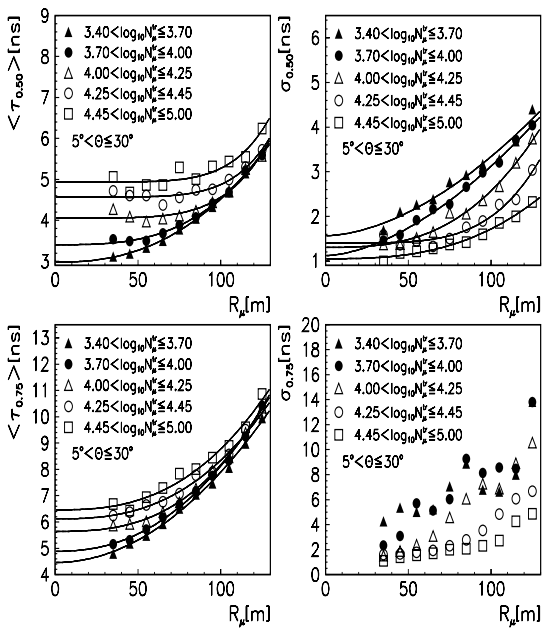

Figure 3: The R_μ dependence of the mean values and of the standard deviations of the median and the third quartile distributions for different ranges of $\log_{10} N_\mu^{tr}$ in the zenith-angle range of $5^o < \theta \leq 30^o$. Full lines are approximations of the time profile by a parabolic shape

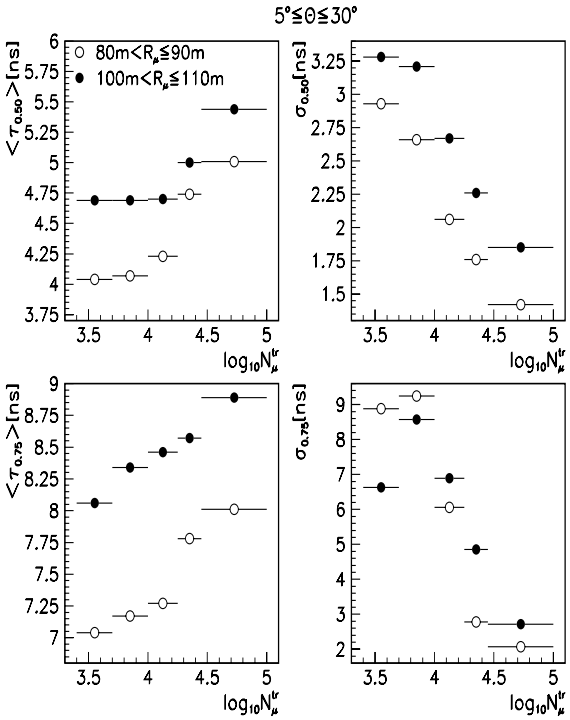

Figure 4: The $\log_{10} N_\mu^{tr}$ dependance of the time moments and their standard deviations for the zenith angle $5^o < \theta \leq 30^o$ and for two ranges of radial distances: $80\ m < R_\mu \leq 90\ m$ and $100\ m < R_\mu \leq 110\ m$

In the present analysis we classified 5 different $\log_{10} N_\mu^{tr}$ ranges covering an energy range from about $8 \cdot 10^{14}$ eV to $3.4 \cdot 10^{16}$ eV. Fig. 3 shows the profiles for different $\log_{10} N_\mu^{tr}$ ranges for the median and the third quartile. It is obvious that the standard deviations of the distributions decrease with increasing primary energy.

Fig. 4 displays the variation of the mean arrival time and of the standard deviations of the median and the third quartile distributions with $\log_{10} N_\mu^{tr}$, indicating a decrease of fluctuations, especially for the last two ranges corresponding to primary energies above the knee. This might be an indication for the appearance of an increasingly heavier primary component in the cosmic rays.

4 Comparison with predictions of Monte-Carlo EAS simulations:

The experimental muon arrival time distributions are compared with simulations of the air shower development, calculated by use of the Monte-Carlo simulation program CORSIKA (Heck et al., 1998). The actual simulation calculations (based on QGSJET model) cover an energy range of $5 \cdot 10^{14} - 1 \cdot 10^{16}$ eV (divided in 5 overlapping energy bins for three mass groups: H = protons, O = CNO group, Fe = heavy group) for an energy distribution of a spectral index of -2.7. They comprise a set of 2000 showers for each case. The response of the KASCADE detector system and the timing qualities have been simulated using the CRES programm, dedicately developed by the KASCADE group on basis of the GEANT code.

Fig. 5 display simulated median distributions of the arrival times for EAS for the $\log_{10} N_\mu^{tr}$ range of 3.7- 4.0. A mass composition H : O : Fe = 4 : 1 : 2 has been adopted. The good agreement of the simulated and the experimental observed distributions (see fig. 1 left side) is remarkable.

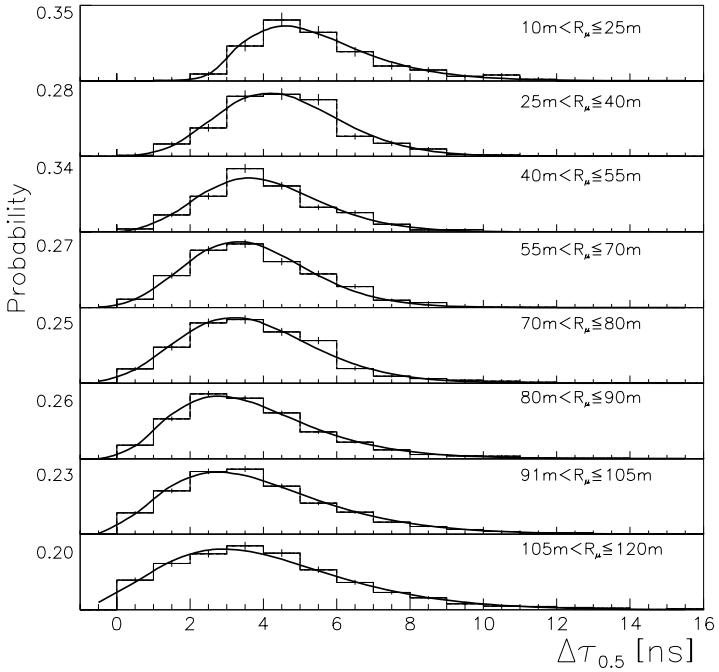

Figure 5: Simulated median muon arrival time distributions, $\Delta\tau_{0.5}$ for different distances from the shower core for a $\log_{10} N_\mu^{tr}$ range of 3.7- 4.0. The lines represents the fit by the Γ-form.

5 Concluding remarks:

With the present studies of the time structure of the EAS muon component inferred from data measured with the KASCADE detector, the phenomenological features of the muon arrival time distributions and of the shower profile and disc thickness are reported. As compared to the results of studies of the charged particle component the time profiles of the EAS muon component appears to be flatter. The time dispersion of the EAS disc conspicuously decreases with higher energies of the primaries, above the knee, possibly indicating a change in the composition. First exploratory comparisons with Monte-Carlo simulations exhibit a remarkably good agreement of the measured data with the theoretical predictions, thus confirming that the CORSIKA simulations describe the longitudinal EAS development quite realistically.

References

Agnetta, G. et al., 1997, Astropart. Phys. 6, 301
Ambrosio, M. et al., 1997, Astropart. Phys., 7, 329
Brancus, I.M. et al., 1998, FZKA-Report 6151, (Forschungszentrum Karlsruhe)
Haungs, A. et al., 1998, FZKA-Report 6105, (Forschungszentrum Karlsruhe)
Heck, D. et al., 1998, FZKA-Report 6019, (Forschungszentrum Karlsruhe)
Klages, H.O. et al., 1997, Nucl. Phys. B (Proc.Suppl.), 52B, 92
Woidneck, C.P. et al., J. Phys. A Math. Gen., 8, 997